Contribution from the Department of Chemistry,
University of California, Santa Barbara, California 93106

Thermal and Photochemical Properties of Some Trans-Disubstituted Tetraammineruthenium(II) Complexes of Aromatic Nitrogen Heterocycles, *trans*-$Ru(NH_3)_4LL'^{n+}$

ELIA TFOUNI[1] and PETER C. FORD*

Received June 18, 1979

Reported are the syntheses and other solution properties of several disubstituted ruthenium(II) amine complexes *trans*-$Ru(NH_3)_4LL'^{n+}$ (L = pyridine (py), L′ = pyrazine (pz), pyrazinium (pzH^+), or 4-acetylpyridine (4-ac-py); L = L′ = pz, pzH^+). The visible range spectra of these species each display two metal-to-ligand charge-transfer absorptions, the lower energy transition being the much more intense. However, the higher energy charge-transfer band is especially prominent when L $\neq$ L′. The aqueous solution basicities of the coordinated pz in these complexes have been determined, and when earlier data are included, the basicity order $Ru(NH_3)_5pz^{2+}$ > *trans*-$Ru(NH_3)_4(py)pz^{2+}$ > *trans*-$Ru(NH_3)_4pz_2^{2+}$ > free pyrazine > *trans*-$Ru(NH_3)_4(pzH)pz^{3+}$ > $Ru(NH_3)_5pz^{3+}$ is obtained. Visible range photolyses of the *trans*-$Ru(NH_3)_4LL'^{n+}$ ions in aqueous solution lead predominantly to the photoaquation of coordinated ammonia. The relative quantum yields of these photoreactions show patterns consistent with the excited-state tuning model proposed to explain photochemical properties of the pentaammine analogues $Ru(NH_3)_5L^{2+}$.

Introduction

Earlier investigations[2] from this laboratory rationalized the photosubstitution reactions of the pentaammine $Ru(NH_3)_5(py\text{-}x)^{2+}$ complexes (py-x is a substituted pyridine) with the following excited state model: These complexes fell into two general categories, those relatively photosubstitution "reactive" complexes with a ligand field state as the lowest energy excited state (ES) and those relatively "unreactive" complexes with a metal-to-ligand charge-transfer (MLCT) state as the lowest ES. The position of the MLCT absorption bands (which dominate the visible spectra of these species) is a sensitive function of substituents on the coordinated pyridine and of solvent, thus variation of either of these parameters allows "tuning" of the photochemical properties.[2,3] The present investigation of trans-disubstituted tetraammine complexes *trans*-$Ru(NH_3)_4LL'$ (where L and L′ are each aromatic nitrogen heterocyclic ligands) was initiated with the goal of examining the generality of this model. In addition, we were cognizant of the observation[4] that the unsymmetrically disubstituted complex *trans*-$Ru(NH_3)_4(py)(4\text{-ac-py})^{2+}$ (4-ac-py = 4-acetylpyridine) displays two strong visible range absorption bands in contrast to the single MLCT band seen[5] for $Ru(NH_3)_5(py\text{-}x)^{2+}$ and reported[6,7] for the symmetrically disubstituted analogues, *trans*-$Ru(NH_3)_4L_2^{2+}$. The question arose whether in the case where two MLCT bands are present the same model would be applicable. Reported here are the photochemical and spectral properties of several such $Ru(NH_3)_4LL'^{n+}$ complexes. Since the pyrazine (pz) was used as a ligand in several of these complexes, we have also examined the aqueous solution acid/base behavior of these complexes.

Experimental Section

Syntheses. All materials were reagent grade and were used without further purification, except for $NaBF_4$ which was recrystallized from water. "Ruthenium trichloride" ($RuCl_3{\cdot}3H_2O$) was the starting material for ruthenium complex syntheses. Doubly distilled water was used throughout this work.

[*trans*-$Ru(NH_3)_4(py)(pz)](BF_4)_2{\cdot}H_2O$ was synthesized following a procedure modified from one previously described for trans-disubstituted Ru(II) complexes.[8,9] A 0.100-mg (0.26 mmol) sample of [*trans*-$Ru(NH_3)_4(SO_4)(py)]Cl$ was dissolved in ~1.5 mL of water and deaerated with argon, trifluoroacetic acid (TFA) (1 drop) and Zn(Hg) (~0.5 g) were added, and the reaction was allowed to proceed ~20 min with continuous argon bubbling. The resulting orange solution was transferred under argon to a deaerated solution of 220 mg (~2.7 mmol) of pyrazine in 0.5 mL of water. After 2 h of reaction time in the dark, the resulting deep red solution was filtered and to this was added a freshly prepared deaerated, almost saturated solution of $NaBF_4$. After cooling of the mixture, dark reddish needles were collected by filtration, washed with methanol and ether, and air-dried. After recrystallization from water, the compound was vacuum dried at room temperature; yield 49%. Anal. Calcd: Ru, 19.44. Found: Ru, 19.31.

[*trans*-$Ru(NH_3)_4(py)(4\text{-ac-py})](BF_4)_2{\cdot}H_2O$ was synthesized following the procedure described by Durante.[4] A 100-mg (0.26 mmol) sample of [*trans*-$Ru(NH_3)_4(SO_4)(py)]Cl$ was dissolved in 1.5 mL of water and a large excess (9 drops) of 4-ac-py added. Argon was bubbled through the solution for 15 min and then 1 drop of TFA and Zn(Hg) (~0.5 g) were added. The mixture was allowed to react in the dark, with continuous bubbling of argon, for about 1 h. The resulting mixture was filtered, and a freshly prepared, deaerated, almost saturated $NaBF_4$ solution was added to the deep red filtrant. After cooling of the mixture, the reddish solid was collected by filtration, washed with ethanol and ether, and vacuum dried at room temperature; yield 80 mg (56%). Anal. Calcd: C, 25.69; H, 4.67; N, 14.98. Found: C, 25.62; H, 4.39; N, 14.68.

[*trans*-$Ru(NH_3)_4(py)_2](BF_4)_2$ was synthesized from [*trans*-$Ru(NH_3)_4Cl_2]Cl$ by the method described by Ford and Sutton,[6] with slight modifications. Anal. Calcd: Ru, 20.17. Found: Ru, 20.03.

[*trans*-$Ru(NH_3)_4(pz)_2](BF_4)_2{\cdot}H_2O$ was synthesized by the same method with slight modifications. A 145-mg (0.53 mmol) portion of [*trans*-$Ru(NH_3)_4Cl_2]Cl$ was suspended in 2.5 mL of water, and the resulting solution was deaerated by argon bubbling for 20 min. To this 1 drop of TFA and Zn(Hg) (~0.5 g) were added, and the reaction was allowed to proceed for 20 min. The solution was then added to a solution of pyrazine (0.5 g, 6 mmol), dissolved in ~1 mL of water, previously deaerated. The mixture was allowed to react in the dark with Ar bubbling for 1 h and then was filtered, and the complex was precipitated by addition of $NaBF_4$ solution. The resulting red crystals were washed with MeOH and ether and air-dried. The product was recrystallized from water and vacuum dried at room temperature; yield 100 mg (35%). Anal. Calcd: Ru, 19.40; C, 18.44;

---

[1] On leave from the Departamento de Química, Faculdade de Filosofia Ciencias e Letras de Ribeirão Preto, Universidade de São Paulo, Ribeirão Preto, São Paulo, Brazil.

[2] (a) Malouf, G.; Ford, P. C. *J. Am. Chem. Soc.* **1977**, *99*, 7213. (b) Malouf, G.; Ford, P. C. *Ibid.* **1974**, *96*, 601.

[3] Ford, P. C. *Rev. Chem. Intermed.*, **1979**, *2*, 267.

[4] Durante, V. A. Ph.D. Dissertation, University of California, Santa Barbara, 1977.

[5] Ford, P. C.; Rudd, De F. P.; Gauder, R.; Taube, H. *J. Am. Chem. Soc.* **1968**, *90*, 1187.

[6] Ford, P. C.; Sutton, C. *Inorg. Chem.* **1969**, *8*, 1544.

[7] Zwickel, A.; Creutz, C. *Inorg. Chem.* **1971**, *10*, 2395.

[8] Marchant, J. A.; Matsubura, T.; Ford, P. C. *Inorg. Chem.* **1977**, *16*, 2160.

[9] Isied, S. S.; Taube, H. *Inorg. Chem.* **1976**, *15*, 3070.

0020-1669/80/1319-0072$01.00/0

Table I. Electronic Spectra of *trans*-Ru(NH$_3$)$_4$LL'$^{n+}$ Complexes and Analogous Ru(NH$_3$)$_5$L^{n+} in Aqueous Solution[a]

complex	λ_{max} (log ϵ)[b] MLCT-1	MLCT-2	intraligand bonds
trans-Ru(NH$_3$)$_4$(py)$_2^{2+}$[c]	423 (4.23)		245 (3.95)
trans-Ru(NH$_3$)$_4$(py)(4-ac-py)$^{2+}$	508 (4.21)	366 (3.48)	271 (3.56), 247 (3.78), 221 (3.91)
trans-Ru(NH$_3$)$_4$(py)(pz)$^{2+}$	474 (4.27)	348 (3.40)	251 (3.99)
trans-Ru(NH$_3$)$_4$(py)(pzH)$^{3+}$[d]	559 (4.31)	~310 (3.18)	272 (3.89), 237 (3.74)
trans-Ru(NH$_3$)$_4$(pz)$_2^{2+}$	486 (4.34)	375 (3.04)	256 (4.13)
trans-Ru(NH$_3$)$_4$(pz)(pzH)$^{3+}$[e]	572 (4.32)	375 (3.11)	273 (3.92), 258 sh (3.85)
trans-Ru(NH$_3$)$_4$(pzH)$_2^{4+}$[f]	626 (4.46)	~440 (2.93)	282 (3.95), 258 sh (3.81)
Ru(NH$_3$)$_5$py^{2+}[g]	407 (3.89)		244 (3.66)
Ru(NH$_3$)$_5$(4ac-py)$^{2+}$[h]	523 (3.97)		271 (3.53), 223 (3.76)
Ru(NH$_3$)$_5$pz^{2+}[h]	472 (4.03)		253 (3.78)
Ru(NH$_3$)$_5$pzH^{3+}[h]	529 (4.08)		272 (3.81)

[a] In dilute aqueous solution except where noted, BF$_4^-$ salts in each case. [b] λ_{max} in nm, ϵ is molar extinction coefficient. [c] Reference 6. [d] In 1.0 N aqueous HCl (μ = 2 M H$^+$, Na$^+$/Cl). [e] In 2 N aqueous HCl. [f] In 10 N aqueous HCl. [g] Reference 5. [h] G. Malouf Ph.D. Dissertation, University of California, Santa Barbara, 1977.

N, 21.51; H, 4.26. Found: Ru, 19.20; C, 18.44; N, 22.01; H, 3.93.

pK_a Determinations. A stock solution of the complex in water was used. The desired series of solutions with different acid (HCl) concentrations were obtained by dilution of measured volumes of the stock solutions of the complex and of HCl. For *trans*-Ru(NH$_3$)$_4$(py)(pz)$^{2+}$, the ionic strength (μ) was fixed at 1.0 M with NaCl. For *trans*-Ru(NH$_3$)$_4$(pz)$_2^{2+}$ μ was fixed at 2.0 M with NaCl for the pK_{a2} determination, whereas it was not possible to do so for the pK_{a1} determination. The pK_a values were determined by using the method described previously,[5,10] where log ($A_{\lambda_1}/A_{\lambda_2}$) is plotted against pH and λ_1 and λ_2 represent absorption maxima for the unprotonated (B) and protonated (BH$^+$) forms, respectively. The pK_a corresponds to the pH where log ($A_{\lambda_1}/A_{\lambda_2}$) equals log $\{(\epsilon(\mathrm{B})_{\lambda_1} + \epsilon(\mathrm{BH}^+)_{\lambda_1})/(\epsilon(\mathrm{B})_{\lambda_2} + \epsilon(\mathrm{BH}^+)_{\lambda_2})\}$. Spectra were recorded with a Cary 118 spectrophotometer thermostated at 25 °C.

Photolysis Procedures. These are quite similar to procedures reported previously.[2a] Irradiations at 449, 479, and 520 nm were carried out by using a 150-W xenon lamp in an Oriel Model 6124 Universal arc lamp source with Oriel interference filter for monochromatization (band-pass ~10 nm), an infrared filter, and a thermostated cell holder. Photolyses at 366 and 405 nm were carried out on an optical train utilizing a PEK 200-W high-pressure mercury short-arc lamp as a light source, an infrared filter, Oriel interference filters, and a thermostated cell holder. Photolyses were carried out in aqueous 0.2 M NaCl, pH ~4 (with HCl) solutions, and with 10^{-3}–10^{-4} M in Ru complex concentration. Ferrioxalate actinometry was used for light intensity measurements at 366 and 405 nm, and Reinecke ion actinometry for 449, 479, and 520 nm.

Solutions for photolysis and dark reactions were prepared and deaerated with purified argon in a Zwickel flask and transferred to the 2.0-cm pathlength quartz cells (V = 6.0 mL) in an all-glass apparatus. During photolysis, the solution was stirred by a small magnetic bar in the cell. All photolyses were carried out at 25.0 ± 0.1 °C. For spectroscopic quantum yield determinations, the reactions under photolysis were monitored periodically by recording the UV–vis spectra on a Cary 118 spectrophotometer. Analogous reactions allowed to react in the dark, under the same conditions of the photolyzed solutions, displayed no observable or just negligible spectral changes. A Sargent-Welch Model NX digital pH meter calibrated against commercial buffers was employed to evaluate pH changes as the result of photolysis. The major cause of such changes was the release of ammonia from the Ru(II) coordination sphere. After photolysis, the pH values of the dark and irradiated solutions were determined, and the quantum yields were calculated from pH differences taking into account the pK_a's of other ligands aquated. The quantities of the organic ligands py, pz, and 4-ac-py released into solution, thermally or photochemically, were determined by ion-exchange chromatography. Typically 5 mL of the photolyzed solution is adjusted to pH 2 with HCl and charged onto a Dowex AG 50W-X-4 column. Pyrazine eluted with 0.01 M HCl solution while pyridine eluted with 0.6 M NaCl (pH 2). For the analysis of the [*trans*-RuA$_4$(py)(4-ac-py)]$^{2+}$ system, the eluent for both py and 4-ac-py was 0.12 M NaCl (pH 4). Concentrations of the ligands in eluent aliquots were determined from absorbance measurements in a 5-cm pathlength cell. The elution conditions and procedures were checked by using stock solution mixtures of py, pz, and 4-ac-py in concentrations near those expected for the photoreaction solutions. Recoveries of ligands in these checks averaged ~95%.

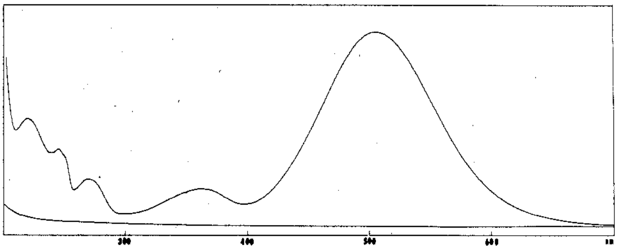

Figure 1. Electronic spectrum in dilute aqueous solution of *trans*-Ru(NH$_3$)$_4$(4-ac-py)py^{2+}.

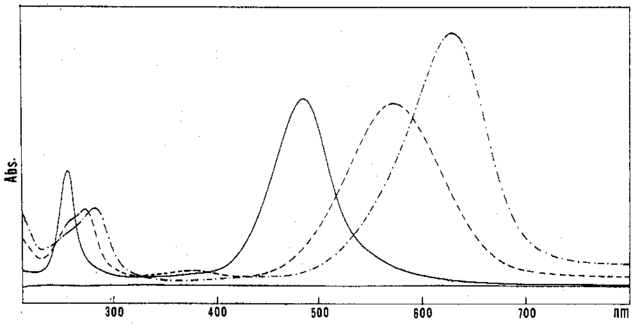

Figure 2. Spectra in aqueous solutions of *trans*-Ru(NH$_3$)$_4$(pz)$_2^{2+}$, *trans*-Ru(NH$_3$)$_4$(pzH)pz^{3+}, and *trans*-Ru(NH$_3$)$_4$(pzH)$_2^{4+}$: —, *trans*-Ru(NH$_3$)$_4$(pz)$_2^{2+}$ in dilute aqueous solution; - - -, *trans*-Ru(NH$_3$)$_4$(pzH)pz^{3+} in 2 M HCl; -·-·- *trans*-Ru(NH$_3$)$_4$(pzH)$_2^{4+}$ in 12 M HCl.

Results and Discussion

Spectra. Table I summarizes the electronic spectral properties of the *trans*-Ru(NH$_3$)$_4$LL'$^{n+}$ ions reported here. The strong absorption bands in the UV region are similar in intensity and position to bands observed in spectra of the free ligands[5] and can be assigned as intraligand π–π^* (IL) in character. The visible spectra of these complexes are dominated in the visible region by one very intense absorption band (MLCT-1, ϵ >10^4 M^{-1} cm^{-1}) plus a less intense band (MLCT-2, ϵ ~10^3 M^{-1} cm^{-1}) apparent at higher energy (Figures 1 and 2). The more intense of these two bands, MLCT-1, has been assigned as a metal to ligand charge-transfer transition for the symmetrically disubstituted ions *trans*-Ru(NH$_3$)$_4$L$_2^{2+}$ (L = py or pz)[6,7] in analogy to spectral assignments[5] of similar absorptions in the pentaammine series Ru(NH$_3$)$_5$L^{2+}. This transition is markedly sensitive to the substituents on the aromatic heterocycles as evidenced by the

---

(10) Clarke, R. E.; Ford, P. C. *Inorg. Chem.* **1970**, *9*, 495.

Table II. Solvent Effects on the Spectrum of $Ru(NH_3)_4(py)(4\text{-ac-py})^{2+\,a}$

solvent	λ_{max} (log ϵ_{max})[b]
CH_3CN	491 (4.23), 366 (3.52), 269 (3.51), 248 (3.77)
CH_3OH	503 (4.21), 373 (3.48), 269 (3.53), 248 (3.77)
H_2O	508 (4.21), 366 (3.48), 271 (3.56), 247 (3.78)
DMF[c]	534 (4.28), 383 (3.53), 273 (3.60), *d*
Me_2SO	543 (4.27), 387 (3.52), 272 (3.61), *d*

[a] Spectra in dilute solution of BF_4^- salt. [b] λ_{max} in nm, ϵ_{max} in L mol^{-1} cm^{-1}. [c] Dimethylformamide. [d] Solvent obscures this region.

red shift of MLCT-1 upon mono- or diprotonation of the bis(pyrazine) complex (Figure 2). As expected for a charge-transfer band, the position of MLCT-1 is also a sensitive function of the solvent medium (Table II).

The less intense visible band MLCT-2 is not seen in the spectrum of *trans*-$Ru(NH_3)_4py_2^{2+}$ and is barely resolvable in the symmetrically disubstituted ions *trans*-$Ru(NH_3)_4pz_2^{2+}$ and *trans*-$Ru(NH_3)_4(pzH)_2^{4+}$. However, the unsymmetrically disubstituted Ru(II) ions, e.g., *trans*-$Ru(NH_3)_4(py)(4\text{-ac-py})^{2+}$ show this band much more distinctly (Figure 1). An ideal example of the behavior is illustrated by Figure 3. Although MLCT-2 has a relatively low intensity for both the $(pz)_2$ and $(pzH^+)_2$ complexes, a far more intense MLCT-2 band is seen for the unsymmetrical $(pz)(pzH^+)$ species. Variation of the solvent medium shifts the position of the MLCT-2 band of *trans*-$Ru(NH_3)_4(py)(4\text{-ac-py})^{2+}$ in a manner comparable to that of MLCT-1 (Table II). For the *trans*-$Ru(NH_3)_4(pz)_2^{2+}$ ion, comparable shifts of MLCT-1 and MLCT-2 bands were noted between the spectra in water (Table I) and in Me_2SO (λ_{max} (log ϵ) 507 (4.37), 395 nm (3.20)) with some enhancement of the MLCT-2 intensity in the latter solvent. The parallel solvent behaviors of MLCT-1 and MLCT-2 lead to the conclusion that the latter is also of metal-to-ligand charge-transfer character.

The origin of MLCT-2 is not obvious. Earlier workers[7] noted the presence of only one visible charge-transfer band[11] (MLCT-1) in the spectra of trans-$Ru(NH_3)_4L_2^{2+}$ but two CT bands of comparable intensity for *cis*-$Ru(NH_3)_4L_2^{2+}$. Zwickel and Creutz[7] rationalized these differences in terms of a qualitative molecular orbital utilizing but one metal dπ orbital plus one π^* orbital from each ligand L. This model does require restrictive assumptions regarding the geometric configurations of the two L's relative to each other (the trans L's were assumed to be coplanar while the cis L's were assumed to be in mutually perpendicular planes) but is reasonably successful in interpreting the band positions. Notably, the Zwickel and Creutz model does predict a second, higher energy MLCT absorption band for the *trans*-$Ru(NH_3)_4L_2^{2+}$ ions which is parity forbidden in the symmetrically disubstituted complexes. According to the parameters of that model, this band is predicted to appear at 399 nm, in reasonable proximity to the ~375-nm position observed. For the unsymmetrical cases, e.g., *trans*-$Ru(NH_3)_4(py)(pzH^+)^{3+}$, the analogous band is no longer strictly forbidden, a possible explanation for the enhanced intensity of this band for the monoprotonated species in comparison to the unprotonated and diprotonated bis(pyrazine) complexes (Figure 3, Table I).

A qualitative interpretation of these spectra can be drawn from a three-π-orbital model similar to that of Zwickel and Creutz.[7] The three orbitals include a dπ from the metal plus one π^* orbital, π_L^* and $\pi_{L'}^*$, from each ligand. Linear combinations of these form three delocalized orbitals Ψ_1, Ψ_2, and Ψ_3 as depicted in Figure 4 for the case where π_L^* is significantly higher in energy than $\pi_{L'}^*$ (e.g., L′ = pz, L = py). In this case, MLCT-1 ($\Psi_2 \leftarrow \Psi_1$) can be viewed as largely charge transfer to L′ in character while MLCT-2 ($\Psi_3 \leftarrow \Psi_1$) is largely charge transfer to L in character. When the energy of $\pi_{L'}$ is further reduced by changing L′, e.g., by protonating the pz of *trans*-$Ru(NH_3)_4(py)(pz)^{2+}$, MLCT-1 should decrease in energy. Given that $b_1 > c_1$ for Ψ_1 and that this will be even more accentuated for the increased energy gap between $\pi_{L'}^*$ and π_L^*, MLCT-2 might be expected to increase in energy, as observed for *trans*-$Ru(NH_3)_4(py)(pzH)^{2+}$. However, this

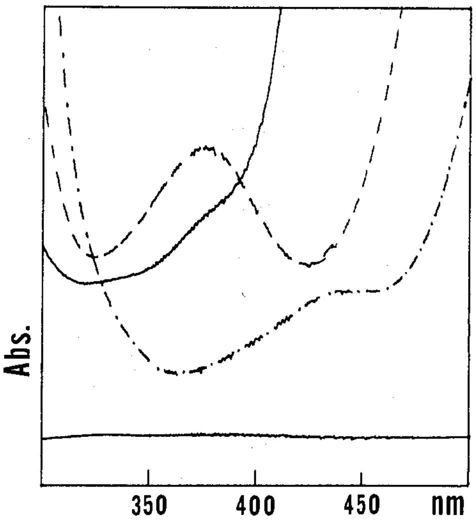

Figure 3. Expanded spectra in regions of the MLCT-2 band for *trans*-$Ru(NH_3)_4(pz)_2^{2+}$ (—, in dilute aqueous solution), *trans*-$Ru(NH_3)_4(pzH)pz^{3+}$ (---, in 2 M HCl), and *trans*-$Ru(NH_3)_4(pzH)_2^{4+}$ (-·-·, in 12 M HCl). The last spectrum was displaced downward for clarity.

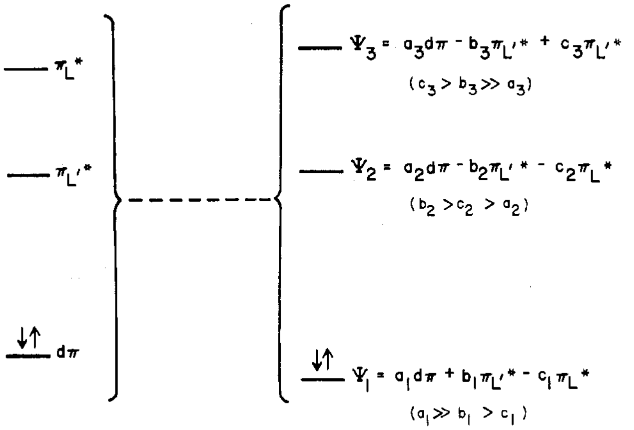

Figure 4. Proposed orbital model for *trans*-$Ru(NH_3)_4LL'^{n+}$.

Table III. pK_a Values[a] for Various Pyrazinium Species

pyrazinium species	pK_a
$Ru(NH_3)_5pzH^{3+}$	2.5[b]
trans-$Ru(NH_3)_4(py)(pzH)^{3+}$	2.0[c]
trans-$Ru(NH_3)(pz)(pzH)^{3+}$	1.5[c]
free pzH^+	0.65[b]
trans-$Ru(NH_3)_4(pzH)_2^{4+}$	−0.6[c] (−1.4)[d]
$Ru(NH_3)_5pzH^{4+}$	−0.8[b] (−2.5)[d]

[a] pK_a equals the −log [Hx] where [Mpz] = [MpzH$^+$]. [b] Reference 5, Hx = $HClO_4$. [c] This work, Hx = HCl. [d] Corrected pK_a value using H_0 value rather than −log [Hx].

---

(11) Note, however, that in an earlier analysis (ref 5) of $Ru(NH_3)_5L^{2+}$ it was suggested that several MLCT absorptions are symmetry allowed. In support of this argument, a magnetic circular dichroism spectrum of $Ru(NH_3)_5py^{2+}$ in acetonitrile solvent indicates the MLCT band of this complex to be composed of at least of two components.[12]

(12) Private communication from Dr. Roger Grinter, University of East Anglia, United Kingdom.

Table IV. Quantum Yields for the Photoaquation Reactions of *trans*-$Ru(NH_3)_4LL'^{2+}$ in Aqueous Solution

L	L'	λ_{irr}[a]	$10^3\Phi_L$,[b] mol/einstein	$10^3\Phi_{L'}$,[b] mol/einstein	$10^3\Phi_{NH_3}$,[c] mol/einstein	$10^3\Phi_{tot}$,[d] mol/einstein
py	py	405	28 ± 2		50 ± 14	78 ± 16
py	py	449	25 ± 2		41 ± 2	66 ± 4
py	pz	366	1.7 ± 0.3	4.3 ± 0.8	34 ± 4	40 ± 5
py	pz	479	0.10 ± 0.01	0.5 ± 0.1	3.6 ± 0.4	4.2 ± 0.5
py	4-ac-py	366	1.4 ± 0.3	1.7 ± 0.6	40 ± 5	43 ± 6
py	4-ac-py	520	<0.05	<0.05	1.0 ± 0.1	1.0 ± 0.1
pz	pz	479	2.7 ± 0.3		2.4 ± 0.6	5 ± 1
py[e]	NH_3[e]	405	45		63	108
py[e]	NH_3[e]	449	49		63	112
4-ac-py[e]	NH_3[e]	405	4.5		27	32
4-ac-py[e]	NH_3[e]	520	0.25		0.9	1.2
pz[e]	NH_3[e]	479	1.4		1.8	3.2

[a] Irradiation wavelength in nm. Photolyses carried out in dilute aqueous solution. $[Ru^{II}] \simeq 10^3$ M, $\mu = 0.2$ (NaCl), pH 4 adjusted with HCl. [b] Quantum yields determined by selective ion-exchange chromatography of photoreleased free ligands, corrected for dark reactions. [c] Quantum yield determined from increases in solution pH (based on the assumption that one NH_3 is released for each H^+ consumed) corrected for pH changes induced by the release of py or pz and for dark reactions. [d] $\Phi_{tot} = \Phi_L + \Phi_{L'} + \Phi_{NH_3}$. [e] Reference 2a.

model is obviously simplistic given the uncertainties regarding configurations of the two ligands relative to each other for the complex in solution, the effects on the absolute energies of this metal t_{2g} orbital as the ligand set is changed,[13] and the suggestion that each MLCT band may represent more than a single transition.[11,12]

pK_a's of Coordinated Pyrazine. The marked changes in the absorption spectra of the ruthenium(II) pyrazine complexes upon protonation of the remote pyrazine nitrogen (Figure 2) allow evaluation of complex pK_a's[5,10] (–log K for eq 1). S-

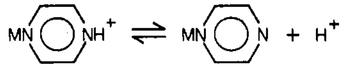

(1)

M = *trans*-$[Ru(NH_3)_4L]^{2+}$

shaped spectral titration curves are obtained by plotting –log [HCl] vs. the logarithm of the ratio of the absorbance at the MpZ λ_{max} to the absorption at the $MpzH^+$ λ_{max} for a series of solutions with the total concentration [Mpz] + [$MpzH^+$] held constant. The pK_a (the –log [HCl] value where [Mpz] = [$MpzH^+$]) is defined by the –log [HCl] value where the curve equals the log of the ratio of ϵ(Mpz) + ϵ($MpzH^+$) at the Mpz λ_{max} divided by ϵ(Mpz) + ϵ($MpzH^+$) at the $MpzH^+$ λ_{max}. The pK_a's so determined are summarized in Table III.

The earlier study[5] of the $Ru(NH_3)_5pzH^{3+}$ ion concluded that the decreased acidity of the Ru(II) coordinated pzH^+ relative to the free ligand could be attributed to π back-bonding delocalizing electron density from the Ru(II) center into the π^* orbitals of the nitrogen heterocycle. Similar effects have been observed with nitrile coordinated cyanopyridine complexes.[10] According to Table III both *trans*-$Ru(NH_3)_4(py)pzH^{3+}$ and *trans*-$Ru(NH_3)_4(pz)pzH^{3+}$ are less acidic than free pzH^+ while *trans*-$Ru(NH_3)_4(pzH)_2^{4+}$ is considerably more acidic. Thus the effect of the trans ligand L on the acidity of Ru(II) coordinated pzH^+ follows the order of increasing acidity NH_3 < py < pz < pzH^+. Since this order is consistent with both the decreasing σ-donor strengths and the increasing π-acceptor strengths of the trans L groups, the individual contributions to the pK_a differences cannot be separately evaluated.

According to the respective pK_a values (Table III), the trans pzH^+ group appears to make the Ru(II) coordinated pzH^+ of *trans*-$Ru(NH_3)_4(pzH)_2^{4+}$ nearly as acidic as the Ru(III) coordinated pzH^+ of $Ru(NH_3)_5(pzH)^{4+}$. However a closer look at these two experiments indicates a greater difference. The *trans*-$Ru(NH_3)_4(pzH)_2^{4+}$ pK_a was measured in aqueous HCl solution where it was found that [Mpz] = [$MpzH^+$] in 4 M HCl while the $Ru(NH_3)_5pzH^{4+}$ pK_a was measured in aqueous $HClO_4$ solution where [Mpz] = [$MpzH^+$] in 6 M $HClO_4$. In strong acid solutions of high concentrations the effective acid strengths are considerably greater than the concentrations and are dependent on the nature of the acids involved. The Hammett acidity function H_0[14] is a more realistic measure of effective acid strengths under these conditions than is –log [HX]. Given that the H_0 values for 4 M HCl and 6 M $HClO_4$ are –1.4 and –2.5, respectively, the *trans*-$Ru(NH_3)_4(pzH)_2^{4+}$ ion appears to be significantly less acidic than the $Ru(NH_3)_5(pzH)^{4+}$ ion.

Photochemistry. Table IV summarizes the quantum yields of the ligand photoaquation observed when the aqueous *trans*-$Ru(NH_3)_4LL'^{2+}$ ions are irradiated in the visible/near-UV ranges. No photooxidation to Ru(III) was seen in this photolysis wavelength range in deaerated solutions. As was found earlier for the pentaammine analogues,[2] following the photolysis-induced decreases in the MLCT absorption bands gives a qualitative estimate of the relative reactivity of a particular complex under the specific conditions. However, since the spectral quantum yields proved uninformative regarding the relative importances of different photoaquation pathways (eq 2), all of the quantum yields listed in Table IV were obtained from the combination of ion exchange and pH measurements. Stereochemistries of Ru(II) products were not determined.

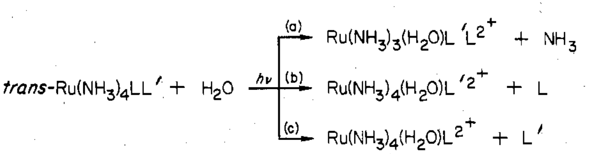

(2)

Notably, there is a close parallel between the photoreaction behavior of the trans tetraammine complexes and similar pentaammine complexes (Table IV and ref 2). The Malouf model[2] for the latter complexes argues that ligand field excited states (LF*) are responsible for ligand labilization. In this model, the character of the lowest energy excited state (either LF* or MLCT*) determines the general pattern of the photoaquation quantum yields. When a LF* is lowest in energy, e.g., aqueous $Ru(NH_3)_5py^{2+}$, initial excitation into the MLCT bands is followed by relatively efficient intersystem crossing/internal conversion to this lowest state. Hence, complexes with this excited state order are relatively "reactive" toward ligand substitution, and their photoreaction quantum yields are generally insensitive to the wavelength of irradiation (λ_{irr}). Complexes having a MLCT* state as the lowest ES are much

---

(13) Templeton, J. L., submitted for publication, private communication from Dr. Templeton.

(14) Paul, M. A.; Long, F. A. *Chem. Rev.* **1957**, *57*, 1.

less photosubstitution active (as expected, since the MLCT* configuration can be represented as a substitution inert Ru(III) coordinated to a reduced ligand center, i.e., Ru^{III}–L).[2] In addition, the photolability observed is sensitive to the irradiation wavelength with quantum yield rising markedly at lower λ_{irr}. This behavior is interpreted as reflecting the population and reactivity of some higher energy LF* states. These reactivity differences plus the proximity of the lower energy LF and MLCT states allow the use of ligand substituents in the "tuning" of photoreaction behavior. Notably, this model has now been used successfully to explain the quantitative photosubstitution behavior of several other types of metal complexes.[3,15]

For the $Ru(NH_3)_5py\text{-}x^{2+}$ complexes, the crossover from "reactive" to "unreactive" behavior comes when the λ_{max} of the MLCT absorption band falls below ~460 nm. Although the data set given in Table IV is limited, a similar pattern is seen for the *trans*-$Ru(NH_3)_4LL'^{2+}$ ions. The bis(pyridine)-complex (λ_{max} 423) is "reactive" with Φ_{tot} independent of λ_{irr}. In contrast, both *trans*-$Ru(NH_3)_4(py)(pz)^{2+}$ (λ_{max}(MLCT-1) = 474 nm) and *trans*-$Ru(NH_3)_4(py)(4\text{-ac-py})^{2+}$ (λ_{max} = 508 nm) display much smaller quantum yields when irradiated at the MLCT-1 maxima and higher quantum yields at shorter wavelengths. Qualitative studies utilizing the spectral changes only (Φ_{spec}) for the latter ions indicate the photoaquation quantum yields follow a smooth gradation for wavelengths between the λ_{irr} values indicated in Table IV. For example, the Φ_{spec} value for *trans*-$Ru(NH_3)_4(py)(4\text{-ac-py})^{2+}$ at λ_{irr} 405 nm is ~$^1/_4$ the value measured at λ_{irr} 366 nm but about 20 times the value at λ_{irr} 520 nm. Thus, there appears to be no special character assignable to the photochemistry resulting when the MLCT-2 band is irradiated.

In another parallel to the pentaammine analogues, the data in Table IV show that the principal photoreaction for *trans*-$Ru(NH_3)_4LL'^{2+}$ is NH_3 aquation regardless of identities of L and L′. For the tetraammine complexes, however, NH_3 photoaquation is unambiguously the result of labilization of ligands cis to the L–Ru–L′ axis. If one assumes that ligand labilization patterns are reflective of the nature of the lowest energy LF* state,[16] the preference for NH_3 labilization implies that the lowest energy LF* state is one that can be qualitatively represented by the one-electron configuration $(d_{xz})^2(d_{yz})^2(d_{xy})^1(d_{x^2-y^2})^1,(d_{z^2})^0$. Given that pyridine is generally considered a weaker σ donor than NH_3,[17] one might expect greater excited-state population in d_{z^2} than in $d_{x^2-y^2}$. This type of behavior is reflected in the photoaquation patterns of the isoelectronic Rh(III) analogues[18] $Rh(NH_3)_5(py\text{-}x)^{3+}$ which photoaquate py-x exclusively under ligand field excitation. The explanation of the different behavior for the Ru(II) complexes must lie with the much greater π back-bonding interaction between the Ru(II) center and π-unsaturated organic ligands. Such interaction may not only lower the energy of d_π orbitals with the appropriate symmetry but also synergetically increase the σ-donor strength of that ligand, the π-acceptor ligands.

Acknowledgment. This work was supported in part by the National Science Foundation. E. T. thanks the Fundacão de Amparo ã Pesquisa do Estado de São Paulo (Foundation for the Support of Research in the State of São Paulo) for financial support. The ruthenium used in these studies was provided on loan by Matthey Bishop, Inc.

Registry No. [*t*-$Ru(NH_3)_4(py)(4\text{-ac-py})](BF_4)_2$, 71964-13-1; [*t*-$Ru(NH_3)_4(py)(pz)](BF_4)_2$, 71964-15-3; [*t*-$Ru(NH_3)_4(py)(pzH)](BF_4)_3$, 71964-16-4; [*t*-$Ru(NH_3)_4(pz)_2](BF_4)_2$, 71964-17-5; [*t*-$Ru(NH_3)_4(py)_2](BF_4)_2$, 71964-18-6; [*t*-$Ru(NH_3)_4(pzH)_2](BF_4)_4$, 71964-19-7; $[Ru(NH_3)_5(4\text{-ac-py})](BF_4)_2$, 71964-20-0; $[Ru(NH_3)_5pz](BF_4)_2$, 41481-91-8; $[Ru(NH_3)_5pzH](BF_4)_3$, 71964-21-1; [*t*-$Ru(NH_3)_4(SO_4)(py)]Cl$, 63251-18-3; [*t*-$Ru(NH_3)_4Cl_2]Cl$, 22327-28-2; *t*-$Ru(NH_3)_4(pzH)pz^{3+}$, 71964-23-3.

---

(15) (a) Wrighton, M. S.; Abrahamson, H. B.; Morse, D. L. *J. Am. Chem. Soc.* **1976**, *98*, 4105. (b) Abrahamson, H. B.; Wrighton, M. S. *Inorg. Chem.* **1979**, *17*, 3385. (c) Figard, J. E.; Peterson, J. D. *Ibid.* **1978**, *17*, 1059.

(16) (a) Vanquickenborne, L. G.; Ceulemans, A. *J. Am. Chem. Soc.* **1977**, *99*, 2208. (b) Wrighton, M. S.; Gray, H. B.; Hammond, G. S. *Mol. Photochem.* **1973**, *5*, 165.

(17) Glerup, J.; Mønsted, O.; Schäffer, C. E. *Inorg. Chem.* **1976**, *15*, 1399.

(18) Petersen, J. D.; Watts, R. J.; Ford, P. C. *J. Am. Chem. Soc.* **1976**, *98*, 3188.

Contribution from the Department of Chemistry,
State University of New York at Stony Brook, Stony Brook, New York 11794

Kinetics and Mechanism of the Forward and Reverse Reactions between (Pyridine)pentaammineruthenium(III) or (4,4′-Bipyridine)pentaammineruthenium(III) and (Ethylenediaminetetraacetato)cobaltate(II)[1]

JAMES PHILLIPS and ALBERT HAIM*

Received June 18, 1979

Kinetic measurements of the forward and reverse reactions for $Ru(NH_3)_5L^{3+} + CoEDTA^{2-} \rightleftharpoons Ru(NH_3)_5L^{2+} + CoEDTA^-$ have been carried out at 25.0 °C, pH 6.0, and ionic strength 0.10 M. For L = pyridine or 4,4′-bipyridine, the rate constants are 32 ± 1 and 77 ± 4 $M^{-1}\,s^{-1}$ (forward reactions) and 236 ± 5 and 156 ± 3 $M^{-1}\,s^{-1}$ (reverse reactions). The mechanisms of these reactions are discussed in the context of Marcus' cross relation for outer-sphere processes corrected for electrostatic effects.

Introduction

The reduction of the d^5 low-spin complex $Fe(CN)_6^{3-}$ by the d^7 high-spin complex $CoEDTA^{2-}$ (EDTA = ethylenediaminetetraacetate) has been studied very extensively.[2-6] The first detectable[2] product (millisecond time scale) of the reaction is the cyano-bridged binuclear complex (EDTA)$Co^{III}NCFe^{II}(CN)_5^{5-}$ in which both metal centers are inert, d^6 low-spin systems. In a time scale of the order of minutes at

---

(1) This work was supported by Grants CHE 7610449 and CHE 79-09253 from the National Science Foundation.

(2) Adamson, A. W.; Gonick, E. *Inorg. Chem.* **1963**, *2*, 129.

(3) Huchital, D. H.; Wilkins, R. G. *Inorg. Chem.* **1967**, *6*, 1022.

(4) Huchital, D. H.; Hodges, R. J. *Inorg. Chem.* **1973**, *12*, 998.

(5) Rosenheim, L.; Speiser, D.; Haim, A. *Inorg. Chem.* **1974**, *13*, 1571.

(6) Huchital, D. H.; Lepore, J. *Inorg. Chem.* **1978**, *17*, 1134.

0020-1669/80/1319-0076$01.00/0